

Original Article

Mycosynthesis of Silver Nanoparticles by *Candida albicans* Yeast and its Biological Applications

Hikmet, R. A^{1*}, Hussein, N. N¹

1. Department of Applied Sciences, Biotechnology Division, University of Technology, Iraq

Received 23 August 2021; Accepted 19 September 2021

Corresponding Author: 100103@uotechnology.edu.iq

Abstract

This study conducted a mycosynthesis of silver nanoparticles (AgNPs) by *Candida albicans* supernatant. The mycosynthesized AgNPs were identified by color visualization, ultraviolet-visible (UV) spectroscopy device, X-ray diffraction (XRD), energy dispersive analysis of X-ray (EDX), field emission scanning electron microscope (FESEM), and zeta potential analysis. The UV-Vis spectroscopy examination has shown the highest absorbance (λ_{max}) at the wavelength of 429 nanometers, which was the indicator of the creation of AgNPs. Furthermore, XRD showed the crystalline structure of AgNPs, and EDX revealed the weight percentage of silver atoms in the sample (82.4%). According to the FESEM, the morphology of AgNPs was spherical, and its size was 40.19 nanometers. Zeta potential analysis indicated that AgNPs were middling stable in the solution, and the zeta potential of AgNPs mycosynthesized by *C. albicans* was -23.02 mV. The cytotoxic effect of AgNPs against a human colon cancer cell line using MTT assay has shown the presence of toxic action against the cells, and no cytotoxic effect appears on the normal cells. The antioxidant activity of AgNPs using DPPH assay demonstrated 17.0%, 29.3%, 48.3%, 67.6%, and 83.6% at concentrations of 6.25, 12.5, 25, 50, and 100 $\mu\text{g/ml}$, respectively. The impact of AgNPs on the chromosomal pattern has also been studied. The importance of this study lies in the possibility of the synthesis of AgNPs using this yeast since most nanoparticle preparation methods utilize molds.

Keywords: AgNPs, Antioxidant, *Candida albicans*, Cytotoxicity, EDX, FESEM, Nanoparticles, UV Spectroscopy, XRD, Zeta Potential

1. Introduction

Nanotechnology is a new domain of science that agrees with the synthesis and application of nanoparticles (NPs). Their size ranged from 1 to 100 nanometers. NPs have been studied extensively due to their special physicochemical features, including antibacterial properties, catalytic activity, anticancer properties, electronic properties, and antioxidant characteristics (1). Using multiple physical, chemical, and biological processes, various metals such as silver (Ag), gold (Au), zinc (Zn), and copper (Cu) have been converted to the nano formula for a wide range of useful uses. Biosynthesis of NPs can be performed

using organisms, such as bacteria, fungi, and plants or their products, which act as reducing and stabilizing agents. Biosynthesis is relatively simple, clean, sustainable, and economical that provides excellent biocompatibility in NPs. The fungi, primarily yeast, represent a suitable option for large-scale green nano production. The mechanism of biosynthesis of NPs by using fungi may be intracellular or extracellular. Several studies demonstrated the biosynthesis of extracellular AgNPs utilizing many fungal species. The second method is most widely used because the releasing of NPs from the cells is simpler and easier than the intracellular mechanism. Moreover,

extracellular biosynthesis required no complex procedures for separation and purification steps. However, to reject fungal remnants and contaminants, the NPs dispersion must be filtered, which can be accomplished using simple filtration, membrane filtration, gel filtration, dialysis, and ultracentrifugation (2-4).

Many studies reported the fungi to represent a good source for the production of AgNPs with cytotoxic activity (5-7). Antioxidants are helpful in the treatment of hypertension and ischemic heart disease. Therefore, the interest in metal NPs in therapies to prevent oxidative damage has grown, and accordingly, they are considered to reduce the apoptotic pathway. The antioxidant properties of AgNPs make them useful in curing diseases (8, 9). This study aimed to conduct an extracellular mycosynthesis of AgNPs by *C. albicans* supernatant and their biological applications.

2. Material and Methods

2.1. Collection and Identification of *C. albicans* Yeast

In total, 50 isolates of *C. albicans* were collected from the patients at Al-Elweya children's teaching hospital in Iraq. Following that, the isolates were diagnosed with Gram stain, microscopic examination, and VITIC2 system. Subsequently, the suitable strain of *C. albicans* was employed for the biosynthesis of AgNPs.

2.2. Preparation of *C. albicans* Supernatant

The fresh characterized colonies of *C. albicans* were cultured in 50 ml of Potato Dextrose Broth medium placed in a falcon tube. 250 ml can ensure aerated circumference for *C. albicans* growth through a clean and sterilized loop inside the hood. In the next stage, the culture was incubated for 48 h in a shaker incubator at 37°C and 150 rpm. After the incubation period, 4000 rpm centrifuge centrifuged the growth medium for 30 min, the sediment was removed, and the supernatant was filtrate by a syringe filter with a diameter of 0.22 µm, and the supernatant was stored at 4°C until it was used. This preparation method was used as previously described with some modifications (10).

2.3 Preparation of Silver Nitrate Solution

To prepare 100 ml of 2mM silver nitrate (AgNO_3) solution, 0.0339 grams of AgNO_3 was dissolved in 100 mL of deionized water. After preparation, the solution was kept in an opaque condition, away from light, to prevent oxidation, and it was used later (11).

2.4. Extracellular Mycosynthesis of Silver Nanoparticles through *C. albicans* Supernatant

10 ml of *C. albicans* supernatant was mixed with 90ml of 2mM silver nitrate solution in a falcon tube and incubated in a shaking incubator at 37°C and 150 rpm for 48 h in dark conditions. After 48 h, the color alteration of the medium should be noticed to detect the formation of AgNPs, which is the first indication of the synthesis of the silver nanoparticles. This mycosynthesis method was used as previously described with some modifications (12).

2.5. Purification of Mycosynthesized Silver Nanoparticles

The reaction mixture that contained AgNPs was put in a centrifuge at a speed of 4000 rpm for 30 min three times with Milli-Q water to reject the medium remains and other impurities. This procedure was recurred at least three times to assure a better separation of AgNPs. This purification method was used as previously described with some modifications (10).

2.6. Characterization of Mycosynthesized Silver Nanoparticles

After 48 h of incubation at a shaking incubator at 37°C and 150 rpm, the color change in the reaction mixture was monitored visually to detect the formation of AgNPs. In the next stage, AgNPs were characterized by UV-Vis spectrophotometer (UV-1650 PC SHIMADZU, Chrom Tech, USA) in the Department of Applied Sciences at the University of Technology in Iraq. Before the UV-Vis spectrophotometer examination, the AgNPs were sonicated for 20 min; moreover, the existence of the greatest absorbance (λ_{max}) and the production of AgNPs were determined using UV-Vis spectra of AgNPs in the region of 200 to 800 nanometers, and deionized water was used as a baseline. X-Ray Diffraction (XRD- Panalytical X Pert

Pro) analysis was used to determine the structural nature of AgNPs. A thin layer of AgNPs has been prepared on glass slides, and the sample was then examined at 40 kV and scanned at 2θ ranging from 10° to 70° . The grain size of AgNPs was calculated using the Scherrer equation as below:

$$D = K \lambda / \beta \cos \theta$$

Where D represents crystallite size, K is the shape factor, λ signifies the X-ray wavelength, β indicates the line broadening at half the maximum intensity, and θ means the Bragg angle. Furthermore, mycosynthesized AgNPs were characterized by field emission scanning electron microscope (FESEM) and energy dispersive analysis of X-ray (EDX) analysis to identify the size, shape, and all the elements that exist in the sample of AgNPs. The sample was spread on a smooth surface of carbon ground and then was coated with a thin layer of gold and examined. Zeta potential analysis was done using Zeta plus analyzer to determine the stability of AgNPs, and the analysis depends on dynamic light scattering measurements assay. The analysis was performed at 25°C , and the dispersion was diluted to an appropriate volume with deionized water (13-15).

2.7. Cytotoxicity Effect of Silver Nanoparticles against HT-29 Cells

To determine the cytotoxic effect of AgNPs, the MTT assay was done using 96-well plates. HT-29 cells, a human colon cancer cell line (HT-29), were seeded at 1×10^4 cells/well. The cells were treated with AgNPs at various concentrations after 24 h or when a confluent monolayer was achieved. After 72 h of treatment, the cell viability was determined by removing the medium adding 28 μL of a 2 mg/mL MTT solution and incubating the cells for 2.5 h at 37°C . Following the removal of the MTT solution, the crystals in the wells were solubilized by adding 130 μL of DMSO (Dimethyl Sulphoxide) and incubating at 37°C for 15 min with shaking. The absorbency was measured at 492 nm using a microplate reader, and the test was conducted in triplicate. The following equation was

used to compute the rate of cell growth inhibition (the percentage of cytotoxicity) (16):

$$\text{Inhibition rate} = A - B/A * 100$$

Where A is the optical density of control, and B signifies the optical density of the samples (17). The cells were seeded into 24-well micro-titration plates at a density of 1×10^5 cells ml^{-1} and cultured for 24 h at 37°C to examine their form under an inverted microscope. The cells were then treated for 24 h to AgNPs at IC_{50} . The plates were stained with crystal violet stain and incubated at 37°C for 10-15 min after the exposure period. The stain was carefully wiped away with tap water until all of the dye was gone. The cells were seen under a $40\times$ magnification inverted microscope with photographs recorded using a digital camera mounted to the microscope (18).

2.8. Antioxidant Properties of Silver Nanoparticles

Antioxidant activity of NPs was measured using stable DPPH radicals with minor adjustments according to (19). The samples were combined with 450 μL of DPPH solution, and 100% ethanol was added to bring the total volume of the combination to one ml. At a concentration of 10 $\mu\text{g}/\text{ml}$, ascorbic acid served as a positive control. For 30 min, both samples and the control were kept in the dark at room temperature. 517 nm was used to determine absorbance. Scavenging activity was calculated using the following equation formula (19):

$$\text{Scavenging}\% = \frac{\text{Absorbance of control} - \text{Absorbance of sample}}{\text{Absorbance of control}} \times 100\%$$

2.9. Effect of Silver Nanoparticles on the Chromosomal Pattern

2.9.1 Blood Specimen

Totally, five milliliters of venous blood were taken from a 25-year-old male who was not exposed to any type of chemical and physical pollution (vocational exposure) and had no genetic diseases (cancers or congenital distortion), no smoking history, and no consumption of any kind of medications for the treatment of chronic and acute diseases during the

sampling period to be ensured that his blood sample was a dependable source of chromosomes in our current study.

2.9.2 Chromosomes Preparation

The preparation technique was followed as described by AbbasHaleem, Abbas (20) by adding 0.5 ml of peripheral blood to 4.5 ml of whole culture medium (RPMI-1640) equipped with 10 µg/ml of phytohemagglutinin that acted as a stimulator, two different concentrations of AgNPs that prepared biologically by *C. albicans* supernatant (0.0, 25, 50) µg/ml, and a test tube containing 0.65 µg/ml of methotrexate as a positive control. The tubes were placed in an incubator in the slanted form at 37°C for 70 h, and colchicine solution was added at a final concentration of 10 µg/ml. The tubes were then returned to the incubator at 37°C for 2 h, after that, the implant was placed in the centrifuge at 2000 rpm speed for 10 min. The precipitate was suspended in 5 mL of hypotonic calcium chloride solution after the supernatant was discarded, which was gradually added with continuous shaking. Subsequently, the tubes were returned to the incubator for another 45 min to remove the red blood cells by exploding them in the potassium chloride solution and swelling of lymphocytes to be ready for the chromosomes preparation.

The tubes were then placed in the centrifuge at a speed of 2000 rpm for 10 min to remove the supernatant, and the sediment was suspended in a cold fixative solution prepared immediately by mixing three parts of absolute methanol with one part of glacial acetic acid. This solution was added as a drop on the wall of the tube with continuous shaking till a volume of approximately 5 ml was obtained. Afterward, the centrifugation process was carried out at a speed of 2000 rpm. This process was reiterated several times till the solution became colorless. The precipitated cells were suspended with 1.5-1 ml of the fixative solution, mixed by a clean and dry Pasteur pipette and got ready for installation on cool and wet slides. A certain size of the prepared cells was taken from above, and at the

height of about 30 cm, seven spaced drops were dropped on the glass slide to obtain a good spreading of the chromosomes for the easy observation of chromosomal changes.

The slides were air-dried in the previous paragraph. After they were completely dried, they were stained with Giemsa stain for two minutes. Furthermore, they were washed with distilled water during which Blast Index (BI) and Mitotic Index (MI) were calculated according to the equations shown below:

$$MI = \frac{\text{Mitotic cells}}{1000 \text{ cell}} \times 100\%$$

$$BI = \frac{\text{stimulated cells}}{1000 \text{ cell}} \times 100\%$$

Chromosomal aberrations= summation of total abnormalities within 25 mitotic cells.

2.10. Statistical Analysis

The data were analyzed in SPSS software (version 24) through the two-way analysis of variance.

3. Results

3.1. Identification of *C. albicans* Isolates

The colonies of *C. albicans* isolates seemed large, round, raised, smooth, glabrous, and white to cream-colored on Sabouraud dextrose agar medium (Figure1). The identification of the isolates was made according to (21). Under microscopic examination with an oil immersion lens and crystal violet stain, the yeast cells exhibited a blue to a purple color indicating that they could retain crystal violet stain as observed in (Figure 2). These microscopic morphological features were recognized according to (22). Furthermore, the isolates of *C. albicans* were diagnosed by the VITIC system.

3.2. Extracellular Mycosynthesis of Silver Nanoparticles

After 48 h of incubation in a shaking incubator in dark conditions at 37°C and 150 rpm, the color change in the reaction mixture was changed from pale yellow to brownish color as shown in figure 3 (A and B).



Figure 1. *C. albicans* colonies on Sabouraud Dextrose Agar medium

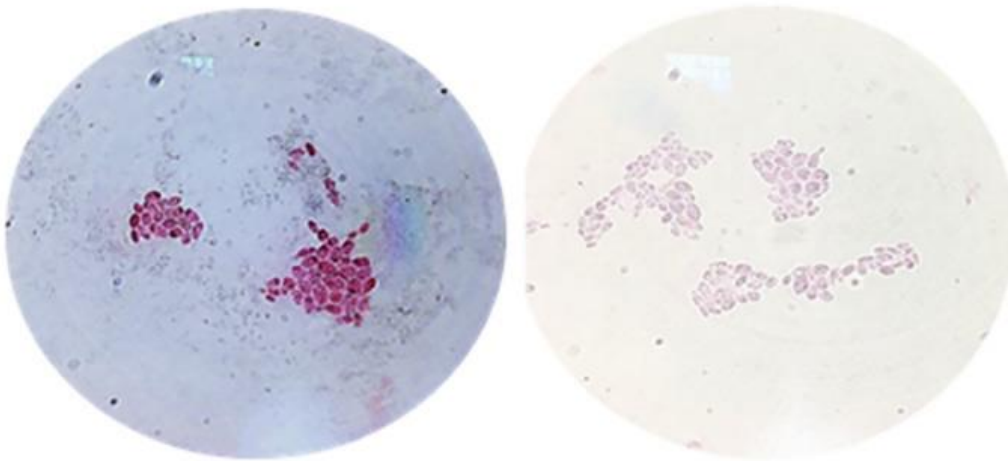


Figure 2. *C. albicans* with Gram stains under a microscope

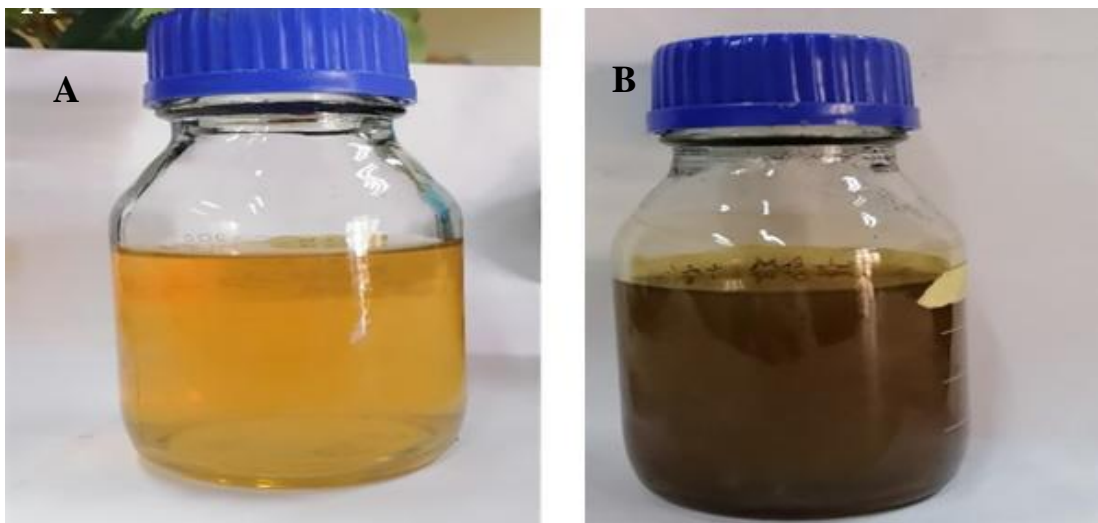


Figure 3. Extracellular mycosynthesis of silver nanoparticles using the supernatant of *C. albicans* (A): before mycosynthesis, (B): after 48 h at 37°C in dark conditions

3.3. Characterization of Silver Nanoparticles

3.3.1. UV-Vis Spectroscopy

The formed AgNPs by *C. albicans* were further specified by UV-vis spectroscopy. The appearance of the highest absorbance (λ_{max}) at the wavelength of 429 nanometers indicated the creation of AgNPs.

3.3.2 X-Ray Diffraction

XRD showed two peaks at 2θ related to Ag nanoparticles, (38.47° and 44.47°) corresponding to

(111) and (200) planes, respectively, when comparing with JCPDS File no. 04-0783 as shown in figure 4.

3.3.3 Energy Dispersive Analysis of X-ray

EDX analysis for AgNPs showed the weight percentage of silver in the sample (82.4%). The presence of a 3eV optical absorbance band implies the existence of AgNPs. At the same time, other signals of Au, C, O, and Cl atoms appear in the graph of EDX as shown in figure 5.

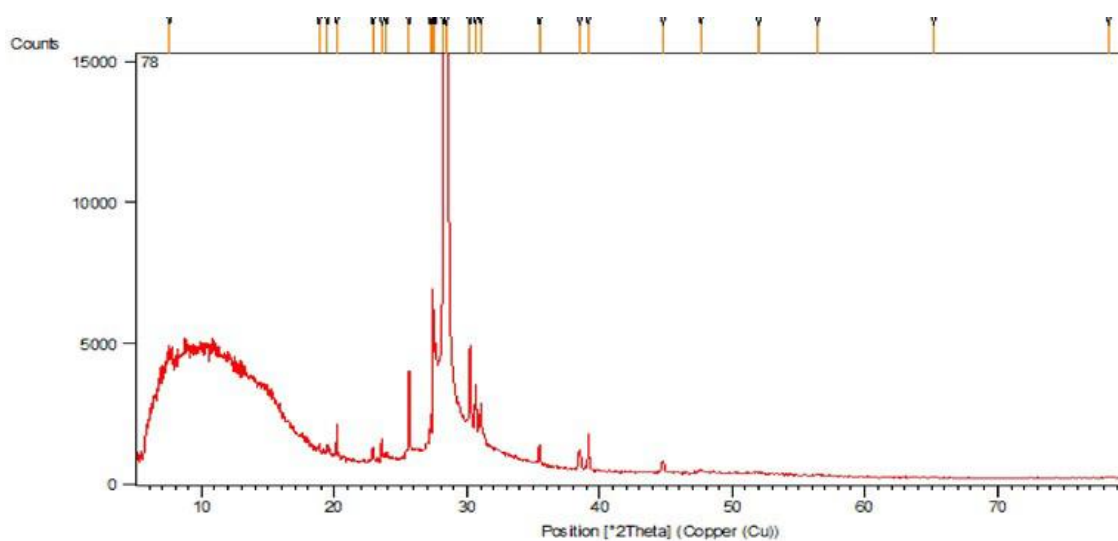


Figure 4. Characterization of silver nanoparticles using X-Ray Diffraction

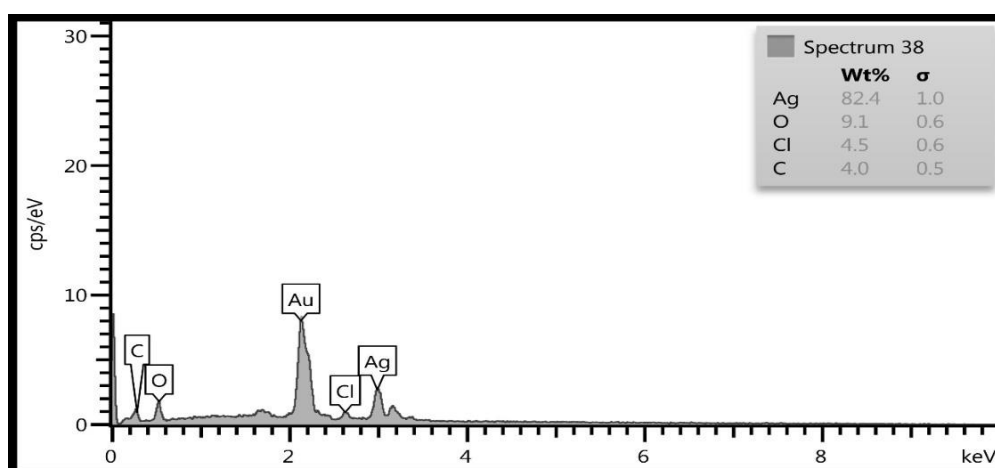


Figure 5. Characterization of silver nanoparticles using the energy dispersive analysis of X-ray analysis

3.3.4 Field Emission Scanning Electron Microscope

The shape and the size of mycosynthesized AgNPs were characterized through FESEM micrographs, and as can be observed in figure 6 (A, B, and C), the morphology of AgNPs was spherical, and its size was 40.19 nm.

3.3.5 Zeta Potential

The Zeta potential of mycosynthesized AgNPs was 23.02 mV with a single peak indicating repulsion among the mycosynthesized AgNPs as can be observed in figure 7.

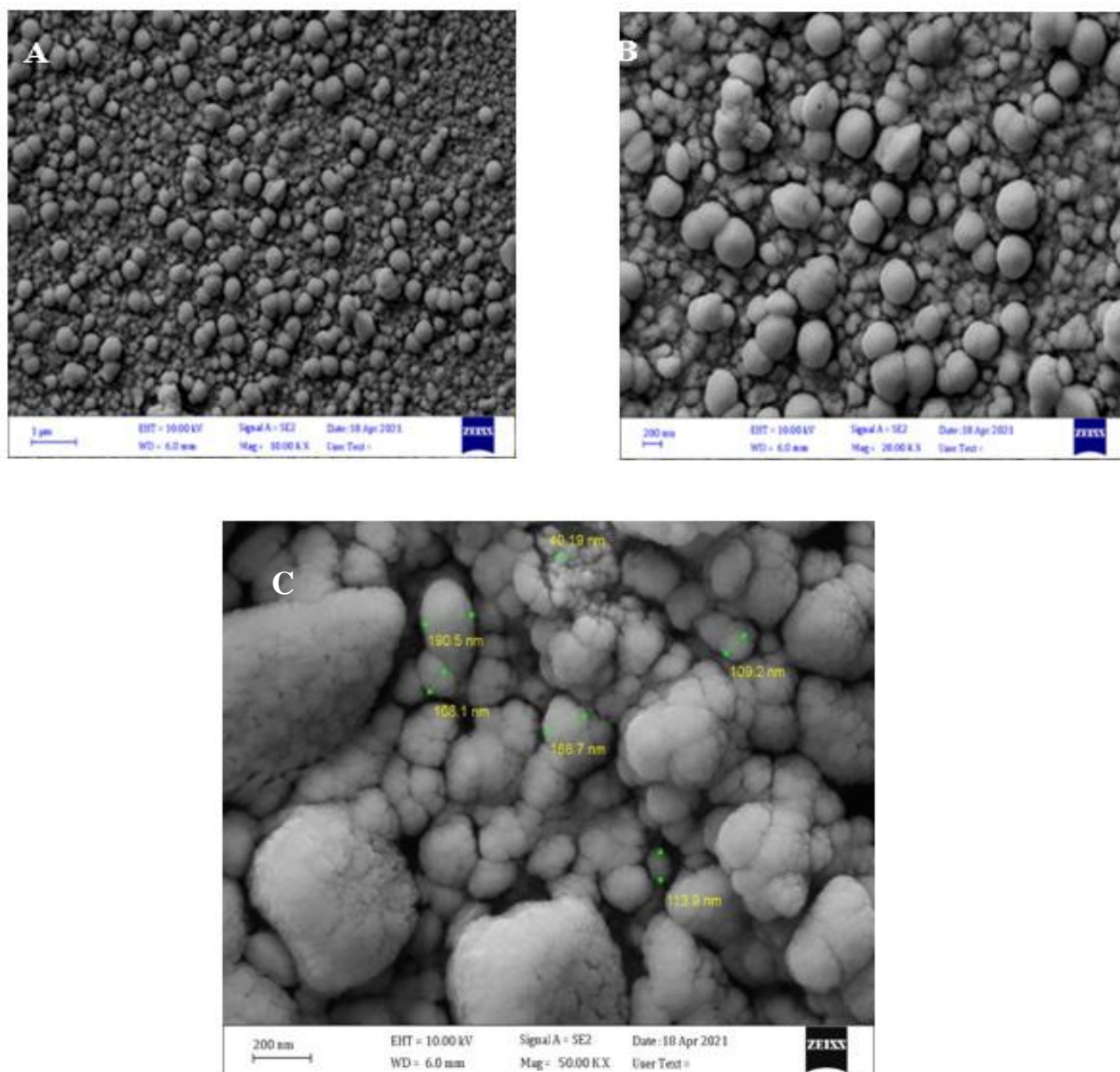


Figure 6. Characterization of silver nanoparticles using the field emission scanning electron microscope analysis at different magnifications

A: at 1µm, **B:** at 200 nm, and **C:** at 200 nm with a different nanoscale bar

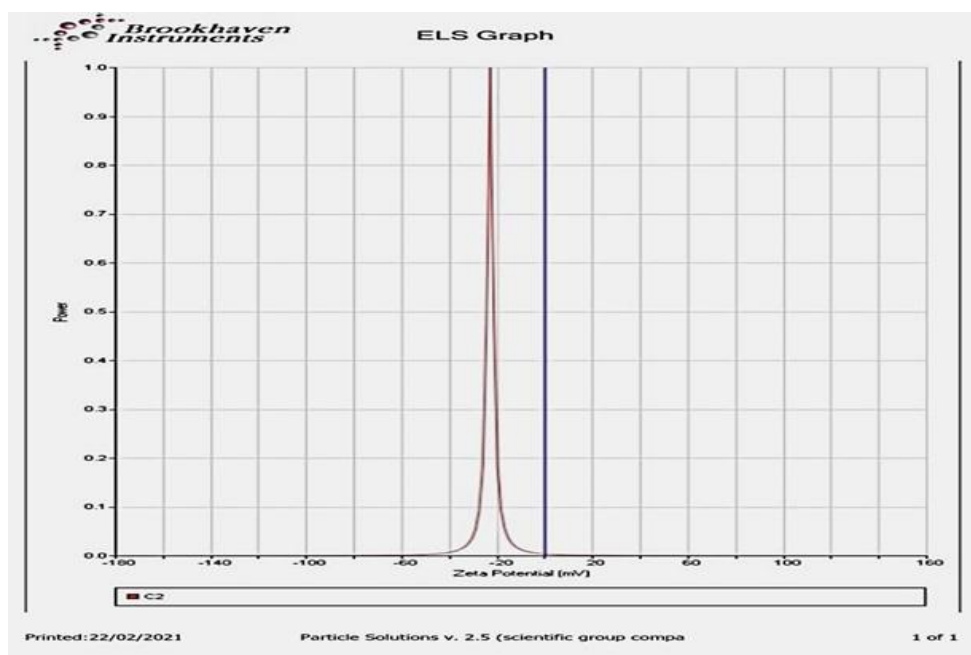


Figure 7. Zeta potential analysis of silver nanoparticles

3.4. Cytotoxicity Effect of Mycosynthesized Silver Nanoparticles against HT-29 Cells

HT-29 cells were used to test the cytotoxicity of mycosynthesized AgNPs. The ability of AgNPs to decrease the proliferation of test cells was used to determine their anti-cancer efficacy. As shown in figures 8 and 9 (A and B), mycosynthesized AgNPs had a highly substantial cytotoxic action against cancer cell lines but not against normal cell lines.

3.5 Antioxidant Properties of Silver Nanoparticles

The DPPH method is an agreeable, fast, and easy method for counting the free radical scavenging activity. Figure 10 shows the mycosynthesized AgNPs that have antioxidant properties. This property is increased by increasing the concentrations of silver nanoparticles. The maximum antioxidant activity was 83.6% at the concentration of 100 $\mu\text{g/ml}$, while the lowest antioxidant activity was 17.0% at the concentration of 6.25 $\mu\text{g/ml}$ (Table 1).

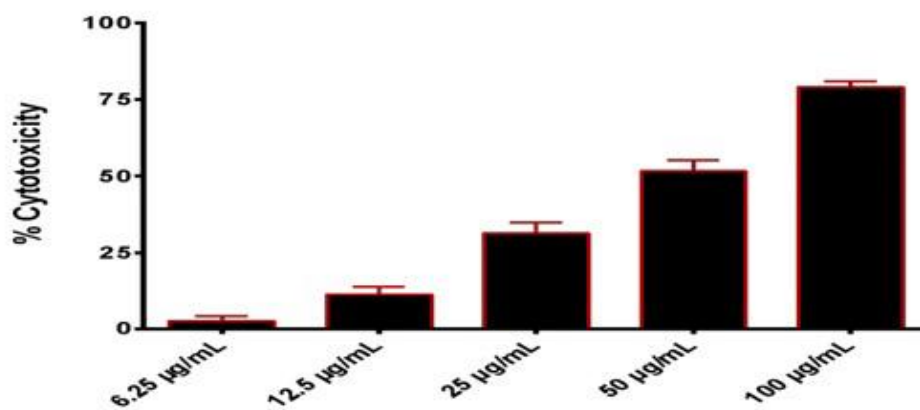


Figure 8. Cytotoxic effect of nanoparticles against HT-29 cells; IC_{50} = 24.10 $\mu\text{g/ml}$

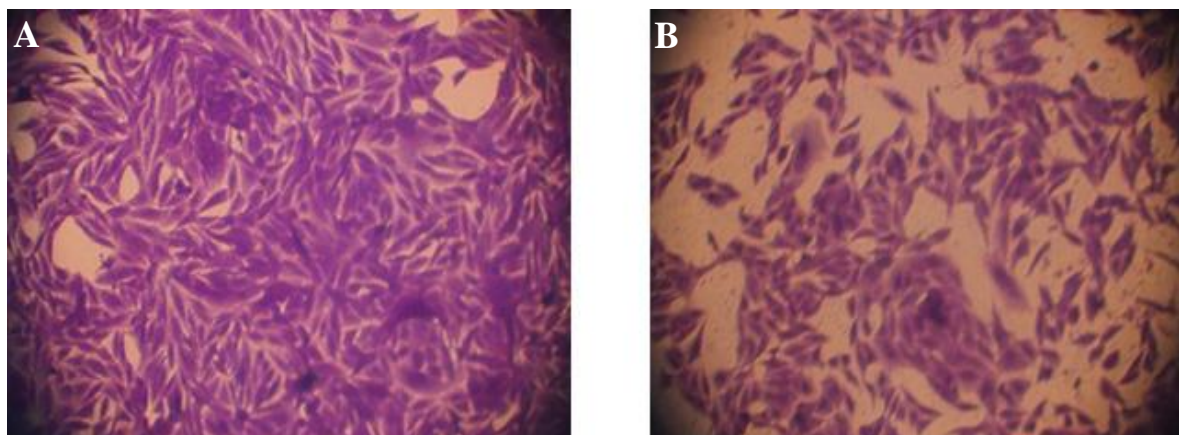


Figure 9. (A) Control untreated HT-29 cells; (B) Morphological changes in HT-29 cell after treated with silver nanoparticles

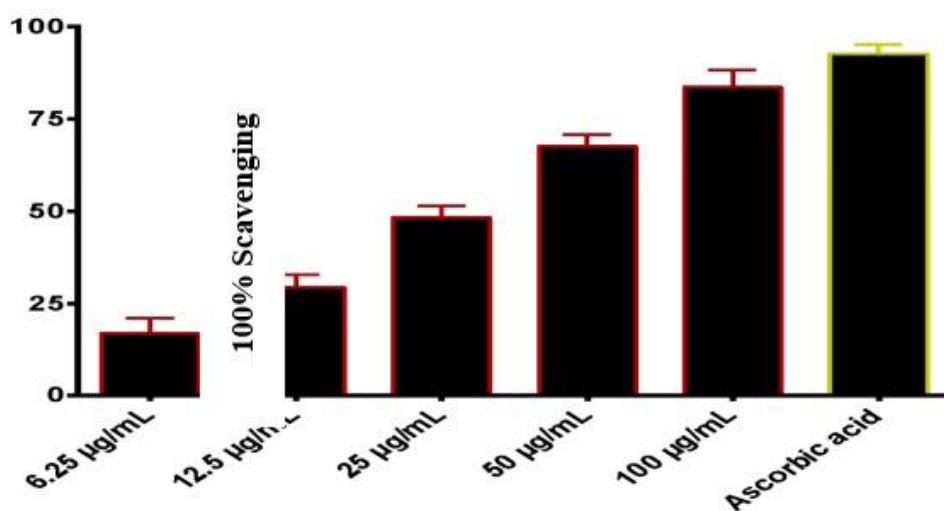


Figure 10. Antioxidant activity of nanoparticles using DPPH assay and the ascorbic acid act as the positive control

Table 1. Antioxidant activity by DPPH method

Silver nanoparticles	
Concentration (µg/ml)	Antioxidant Activity (%)
6.25	17.0
12.5	29.3
25	48.3
50	67.6
100	83.6

3.6. Chromosomal Analysis

Table 2 shows that the total chromosomal abnormality (TCA) is directly proportional to an increase in the concentration of AgNPs. The

decrease in the BI and MI indicators was the result of cell death or cessation at some stages of interphase and the effect of AgNPs on their cleavage.

Table 2. Chromosomal aberrations induced in peripheral blood lymphocytes treated with silver nanoparticles

Silver nanoparticles			
Concentration ($\mu\text{g/mL}$)	BI	MI	TCA
0.0	66.22	1.25	0.24
25	61.18	1.02	0.33
50	59.13	0.88	0.36
Methotrexate0.65	16.55	0.11	0.52

BI=Blast Index, MI=Mitotic Index, TCA=Total Chromosomal Aberrations

4. Discussion

The color alteration in the mycosynthesis of AgNPs by *C. albicans* was the first indicator of the formation of AgNPs because of the reduction of Ag ions and Plasmon resonance. These findings are consistent with those of a prior study conducted by Mourad Magdi, Mourad (23). In the characterization of AgNPs using a UV-vis spectrophotometer, the appearance of λ_{max} at the wavelength of 429 nanometers indicated the formation of AgNPs, which was because of the phenomenon of the surface Plasmon resonance that occurred due to the excitation of the surface Plasmon present on the outer surface of the AgNPs. This got excited due to the applied electromagnetic field. These findings are quite similar to the results of a study conducted by Bhat and Nayak (10) who discovered that AgNPs biosynthesized by *C. albicans* had an absorption peak at 430 nm. The appearance of two peaks at 2θ (38.47° and 44.47°) in the XRD analysis are related to AgNPs and the crystalline nature of mycosynthesized AgNPs. The crystallite size was 58.5 nm using the Scherrer equation. These findings are consistent with the results of a study performed by Abdehghah, Khodavandi (24) who discovered that *C. albicans* biosynthesizing AgNPs had a crystalline form. The benefit of determining the size

of nanoparticles depends on their effectiveness and behavior as antibacterial. As it is known, nanoparticles increase their effectiveness at smaller sizes.

In the spectrum of EDX analysis, signals of Au, C, O, and Cl atoms may have been originated from the biomolecules found on the surface of the AgNPs and the appearance of Au in the EDX analysis of AgNPs due to the presence of substrate over which the NPs sample was held during FESEM microscopy. These results are in line with the findings of the previous studies (25, 26). This weight percentage is close to that in a study carried out by Dhabalia, Ukkund (27) who reported the weight percentage of AgNPs as 85.7%. The spherical form of mycosynthesized AgNPs was revealed by FESEM, and their size was 40.19 nm.

This is less than the average size of AgNPs biosynthesized by *C. albicans* as reported by Bhat, Nayak (10). They discovered that the average size of AgNPs biosynthesized by *C. albicans* was between 60.88 and 65.57 nm in their study. The shape and the size of mycosynthesized AgNPs that were gained from this study were in agreement with those in the study carried out by Dhabalia and Ukkund (27). They reported the average size of AgNPs that were biosynthesized by *C. albicans* as 30-70 nm with a spherical shape. Moreover, these results are consistent

with the findings of the prior studies that used other fungi (28, 29). The negative Zeta potential of mycosynthesized AgNPs was discovered indicating dissonance among green produced AgNPs and raising the stability of the compound. Because of the moderate negative Zeta potential value of AgNPs, it is obvious that they are intermediate poly distributed in the sample, and the electrostatic repulsive force between them leads to a poor inhibition of nanoparticle clotting. In addition, AgNPs exhibit a state of primary instability in the solution. These results are consistent with the findings in the earlier studies conducted by Niknejad, Nabili (30), Kim, Kuk (31), as well as Elamawi, Al-Harbi (32).

Bio-manufactured AgNPs have been used on various types of cancerous cells, such as skin cancer cells. It has been observed that tumor progression is inhibited by AgNPs and controls the progression of the disease without causing toxicity to normal cells. This study finds that AgNPs have the ability to suppress the growth of HT-29 cell lines, and this effect is concentration-dependent manner. The IC_{50} was 24.10 $\mu\text{g/ml}$. These results are consistent with the findings of the earlier studies conducted by Ismail, Ahmed (33), as well as Yehia and Al-Sheikh (34).

Many cells produce reactive oxygen species (ROS), including single oxygen, irritating carbonyl ($\text{C}=\text{O}$), and hydrogen peroxide, which can damage cell components, such as proteins, lipids, and DNA resulting in cell death. The use of AgNPs to combat ROS yielded outstanding results. Antioxidants are well-known for their ability to scavenge free radicals and protect the body from a variety of ailments, including heart disease and cancer. The use of AgNPs to combat ROS yielded novel outcomes (8). The mycosynthesized AgNPs by *C. albicans* show maximum antioxidant activity (83.6%) at the concentration of 100 $\mu\text{g/ml}$. This is in line with the findings of other studies conducted by Menon, Agarwal (35), as well as Vorobyova, Vasyliiev (36).

The study finds that AgNPs affect chromosomal patterns through an increase in the TCA index, and the reason for this may be the effect of the toxin that binds to cell receptors located in the plasma membrane and leads to the process of sensing and contributing to the response process to these substances and stimulating the systems responsible for the process of toxicity machine. The effect of any cleaved material is by activating the genetic material of the cell since the genes responsible for growth are activated to give orders to enter the mitotic cycle within a specific period that depends on the cell type and the efficiency of the stimulating material in the presence of AgNPs. The cell will not be able to go through its four phases during the normal period of division. It may have exceeded the first mitotic cycle; however, it will not be able to pass in the second and third (37, 38).

5. Conclusion

The findings of this study reveal that mycosynthesized AgNPs can be made in a simple, safe, cost-effective, and environmentally friendly way by employing yeast *C. albicans*, compared to other methods of preparing AgNPs, such as physical and chemical methods. AgNPs showed a cytotoxic effect on the HT-29 using the MTT assay, and no cytotoxic effect appeared on normal cells. Furthermore, AgNPs showed antioxidant activity using the DPPH assay. Because of their special characteristics of silver and nano size, mycosynthesized AgNPs look promising in pharmaceutical, biological, and other fields, providing that safety data is generated to verify their safety while excluding the possibility of toxicity.

Authors' Contribution

Study concept and design: R. A. H.

Acquisition of data: N. N. H.

Analysis and interpretation of data: R. A. H.

Drafting of the manuscript: R. A. H.

Critical revision of the manuscript for important intellectual content: N. N. H.

Statistical analysis: N. N. H.

Administrative, technical, and material support: R. A. H.

Ethics

All procedures performed in this study involving human participants were in accordance with the ethical standards of the University of Technology, Iraq.

Conflict of Interest

The authors declare that they have no conflict of interest.

Grant Support

No funding support by our institution was provided. The authors are responsible for their funding support.

Acknowledgment

The authors are grateful to the Department of Applied Sciences Laboratories, University of Technology, Baghdad, Iraq, for providing experimental support.

References

- Al-Tae E. Effect of silver nanoparticles synthesized using leaves extract of Olive on histopathological and cytogenetic effects in Albino mice. *Iraqi J Agric Sci.* 2020;51(5):1448-57.
- Atwan Q, Hayder N. Eco-friendly synthesis of Silver nanoparticles by using green method: Improved interaction and application in vitro and in vivo. *Iraqi J Agric Sci.* 2020;51:201-16.
- Gudikandula K, Vadapally P, Charya MS. Biogenic synthesis of silver nanoparticles from white rot fungi: Their characterization and antibacterial studies. *Open Nano.* 2017;2:64-78.
- Qidwai A, Kumar R, Shukla S, Dikshit A. Advances in biogenic nanoparticles and the mechanisms of antimicrobial effects. *Indian J Pharm Sci.* 2018;80(4):592-603.
- Elshawy OE, Helmy EA, Rashed LA. Preparation, characterization and in vitro evaluation of the antitumor activity of the biologically synthesized silver nanoparticles. *Adv Nano.* 2016;5(02):149.
- Hu X, Kandasamy Saravanakumar TJ, Wang M-H. Mycosynthesis, characterization, anticancer and antibacterial activity of silver nanoparticles from endophytic fungus *Talaromyces purpureogenus*. *Int J Nanomedicine.* 2019;14:3427.
- Salaheldin TA, Husseiny SM, Al-Enizi AM, Elzatahry A, Cowley AH. Evaluation of the cytotoxic behavior of fungal extracellular synthesized Ag nanoparticles using confocal laser scanning microscope. *Int J Mol Sci.* 2016;17(3):329.
- Jogaiah S, Kurjogi M, Abdelrahman M, Hanumanthappa N, Tran L-SP. Ganoderma applanatum-mediated green synthesis of silver nanoparticles: Structural characterization, and in vitro and in vivo biomedical and agrochemical properties. *Arab J Chem.* 2019;12(7):1108-20.
- Pellegrino D. Antioxidants and cardiovascular risk factors. *Diseases.* 2016;4(1):11.
- Bhat MA, Nayak B, Nanda A. Evaluation of bactericidal activity of biologically synthesised silver nanoparticles from *Candida albicans* in combination with ciprofloxacin. *Mater Today: Proc.* 2015;2(9):4395-401.
- Shameli K, Ahmad MB, Zamanian A, Sangpour P, Shabanzadeh P, Abdollahi Y, et al. Green biosynthesis of silver nanoparticles using *Curcuma longa* tuber powder. *Int J Nanomedicine.* 2012;7:5603.
- Jalal M, Ansari MA, Alzohairy MA, Ali SG, Khan HM, Almatroudi A, et al. Biosynthesis of silver nanoparticles from oropharyngeal *Candida glabrata* isolates and their antimicrobial activity against clinical strains of bacteria and fungi. *Nanomaterials.* 2018;8(8):586.
- Hussein N, Muslim A. Detection of the antibacterial activity of AgNPs biosynthesized by *Pseudomonas aeruginosa*. *Iraqi J Agric Sci.* 2019;50(2):617-25.
- Ibrahim O, Abed A, Yahea N. Evaluation of Biological Activity of Greenly Synthesized Silver Nanoparticles Using Aloe Vera Gel Extract As Antibacterial Agent In-Vitro and In-Vivo. *Iraqi J Agric Sci.* 2020;51(6):1706-15.
- Kadhun M, Hussein N. Detection of The Antimicrobial Activity of Silver Nanoparticles Biosynthesized By *Streptococcus Pyogenes* Bacteria. *Iraqi J Agric Sci.* 2020;51(2):500-7.
- Al-Ziaydi AG, Hamzah MI, Al-Shammari AM, Kadhim HS, Jabir MS, editors. The anti-proliferative activity of D-mannoheptulose against breast cancer cell line through glycolysis inhibition. *AIP Conference Proceedings: AIP Publishing LLC; 2020.*
- Al-Ziaydi AG, Al-Shammari AM, Hamzah MI, Kadhim HS, Jabir MS. Newcastle disease virus suppress

- glycolysis pathway and induce breast cancer cells death. *Virusdisease*. 2020;31(3):341-8.
18. Jabir MS, Hussien AA, Sulaiman GM, Yaseen NY, Dewir YH, Alwahibi MS, et al. Green synthesis of silver nanoparticles from *Eriobotrya japonica* extract: a promising approach against cancer cells proliferation, inflammation, allergic disorders and phagocytosis induction. *Artif Cells Nanomed Biotechnol*. 2021;49(1):48-60.
 19. Al-Rashid T, Jabi M, Nayef U. Preparation and characterization of colloidal Au-ZnO Nanocomposite via laser ablation in deionized water and study their antioxidant activity. *J Phys Conf Ser*. 2021;1795:012057
 20. Haleem AM, Abbas RH, Jawad MA, Alberaqqdar F. Cytotoxic effects of titanium dioxide nanoparticles synthesized by laser technique on peripheral blood lymphocytes and hep-2 Cell Line. *Toxicol Environ Health Sci*. 2019;11(3):219-25.
 21. Bhavan PS, Rajkumar R, Radhakrishnan S, Seenivasan C, Kannan S. Culture and Identification of *Candida albicans* from Vaginal Ulcer and Separation of Enolase on SDS-PAGE. *Int J Biol*. 2010;2(1):84.
 22. Ellis DH, Davis S, Alexiou H, Handke R, Bartley R. Descriptions of medical fungi: University of Adelaide Adelaide; 2007.
 23. Magdi HM, Mourad MH, El-Aziz M. Biosynthesis of silver nanoparticles using fungi and biological evaluation of mycosynthesized silver nanoparticles. *Egypt J Exp Biol (Bot)*. 2014;10(1):1-12.
 24. Abdehghah IB, Khodavandi A, Shamsazar A, Negahdary M, Jafarzadeh M, Rahimi G. In vitro antifungal effects of biosynthesized silver nanoparticle by *Candida albicans* against *Candida glabrata*. *Biomed Res (India)*. 2017;28:2870-6.
 25. Gowramma B, Keerthi U, Rafi M, Rao DM. Biogenic silver nanoparticles production and characterization from native stain of *Corynebacterium* species and its antimicrobial activity. *Biotech*. 2015;5(2):195-201.
 26. Siddiqi KS, Husen A, Rao RA. A review on biosynthesis of silver nanoparticles and their biocidal properties. *J Nanobiotechnology*. 2018;16(1):1-28.
 27. Dhabalia D, Ukkund SJ, Syed UT, Uddin W, Kabir MA. Antifungal activity of biosynthesized silver nanoparticles from *Candida albicans* on the strain lacking the CNP41 gene. *Mater Res Express*. 2020;7(12):125401.
 28. Guilger-Casagrande M, Lima Rd. Synthesis of silver nanoparticles mediated by fungi: a review. *Front Bioeng Biotechnol*. 2019;7:287.
 29. Hulikere MM, Joshi CG. Characterization, antioxidant and antimicrobial activity of silver nanoparticles synthesized using marine endophytic fungus-*Cladosporium cladosporioides*. *Process Biochem*. 2019;82:199-204.
 30. Niknejad F, Nabili M, Ghazvini RD, Moazeni M. Green synthesis of silver nanoparticles: advantages of the yeast *Saccharomyces cerevisiae* model. *Curr Med Mycol*. 2015;1(3):17.
 31. Kim JS, Kuk E, Yu KN, Kim J-H, Park SJ, Lee HJ, et al. Antimicrobial effects of silver nanoparticles. *Nanomed Nanotechnol Biol Med*. 2007;3(1):95-101.
 32. Elamawi RM, Al-Harbi RE, Hendi AA. Biosynthesis and characterization of silver nanoparticles using *Trichoderma longibrachiatum* and their effect on phytopathogenic fungi. *Egypt J Biol Pest Control*. 2018;28(1):1-11.
 33. Ismail AF, Ahmed MM, Salem AA. Biosynthesis of silver nanoparticles using mushroom extracts: induction of apoptosis in HepG2 and MCF-7 cells via caspases stimulation and regulation of BAX and Bcl-2 gene expressions. *J Pharm Biomed Sci*. 2015;5(1):1-9.
 34. Yehia RS, Al-Sheikh H. Biosynthesis and characterization of silver nanoparticles produced by *Pleurotus ostreatus* and their anticandidal and anticancer activities. *World J Microbiol Biotechnol*. 2014;30(11):2797-803.
 35. Menon S, Agarwal H, Kumar SR, Kumar SV. Green synthesis of silver nanoparticles using medicinal plant *Acalypha indica* leaf extracts and its application as an antioxidant and antimicrobial agent against foodborne pathogens. *Int J Appl Pharm*. 2017;9(5):42-50.
 36. Vorobyova V, Vasyliov G, Skiba M. Eco-friendly "green" synthesis of silver nanoparticles with the black currant pomace extract and its antibacterial, electrochemical, and antioxidant activity. *Appl Nanosci*. 2020;10(12):4523-34.
 37. Carpenter DO, Arcaro K, Spink DC. Understanding the human health effects of chemical mixtures. *Environ Health Perspect*. 2002;110(1):25-42.
 38. Dabaghi A, Bagheri M. The Issue of Translating Culture: A Literary Case in Focus. *Theory Pract Lang Stud*. 2012;2(1).